IJBPAS, November, 2020, 9(11): 2951-2964

ISSN: 2277–4998

International Journal of Biology, Pharmacy and Allied Sciences (IJBPAS)

'A Bridge Between Laboratory and Reader'

www.ijbpas.com

DESIGN OF POTENTIAL RNAi MOLECULES FOR TARGETING COVID-19

JAYA LAKSHMI N AND JABALIA N*

Amity University, Uttar Pradesh, India

***Corresponding Author: Neetu Jabalia: E Mail: njabalia@gmail.com**

Received 4th June 2020; Revised 15th June 2020; Accepted 25th June 2020; Available online 1st Nov. 2020

https://doi.org/10.31032/IJBPAS/2020/9.11.5245

ABSTRACT

Today our world is trapped under an evasive pandemic called COVID 19 which has claimed upto 503k lives and still counting. COVID 19 is a highly communicable disease caused by a subfamily of a coronavirinae specifically known as SARS CoV-2 of beta coronavirus family. Since the scale of this new disease is humongous a novel vaccine for the effective treatment of the infected patients is yet to be developed. This paper gives a positive direction towards vaccine development by utilizing RNAi as medium to block the access of the virus into the human host. The last section highlights computational approach towards designing potential RNA interference molecules targeting the surface glycoprotein of SARS CoV-2 virus.

Keywords: COVID 19, SARS CoV-2, RNAi, Surface glycoprotein

INTRODUCTION

COVID19 is a global outbreak caused by SARS-CoV2 virus that is believed to be originated in Huanan Seafood Wholesale Market of Wuhan in South China. COVID19 majorly affects the entire respiratory tract to develop varying levels of pneumonia. Fever (87.9%) and cough (67.7%) are the most widely observed symptoms of COVID19 **[1, 2]**. Among the structural components of Coronaviruses, the Surface glycoprotein(S) is a class 1 homotrimeric 150kDa (approx.) protein which contains two subunits S1 and S2 namely.S protein helps in forming distinct spikes/crown on the surface of virus which helps it to attach to the host cell by binding to its receptors **[3]**. The mechanism of action can be briefly described as the binding of S1 to host cellular receptor angiotensin converting enzyme 2 facilitating the activation of renin angiotensin system which causes lung damage triggering a cascade of processes that include vascular permeability elevation and alterations in the epithelial

cells of our alveoli **[4-7]**. Currently there is no vaccine or specific drug targeting SARS CoV2. Eventhough drugs such as Remdesivir, Hydroxychloroquine are being used to control COVID 19 but they come with their share of side effects and do not provide a permanent solution **[8]**.

RNAi is a regulatory mechanism responsible for invading viruses by innate defence system and for gene regulation which is schematically explained in Figure 1. Past studies have shown that RNAi has played a significant role in targeting coronaviruses. Gene therapy in SARS associated virus has shown a 92% reduction in viral titer using siRNA mediated gene silencing. **[9]** Hasan *et al* computationally predicted human micro RNAs for targeting MERS-CoV Genome **[10]**. DsRNA from transcribed genes or those presented artificially are processed into smaller molecules called siRNA by RNAase enzymes like DICER within the cytoplasm **[11]**. The siRNA activates the RNA-induced silencing complex (RISC). An endonuclease enzyme called as Argonaute 2 (AGO2) a part of the RISC is responsible for cleaving the passenger strand of the siRNA while its guide strand remains linked to the RISC. Next, the guide strand directs the activated RISC to bind to the target messenger RNA (mRNA) which is cleaved by AGO2.

Finally, the guide strand that further binds to the entirely complementary target mRNA, thereby resulting in its gene silencing via repression **[12]**. In a similar fashion the pre-miRNA is transported from nucleus to the cytoplasm where DICER cleaves it to form a long mi-RNA duplex which associates with the RISC complex to form mi-RISC. This duplex undergoes unwinding so that the passenger strand gets removed. This mature ss microRNA so formed directs the micro-RISC binding to its target messenger RNA in partly complementary fashion. Finally end product of the cascade is targeted gene silencing that is ensued from translational repression, messenger RNA degradation or its cleavage **[13, 14]**.

In this study the major objective was to design RNAi molecules targeting the surface glycoprotein of SARS CoV2 genome that will result in its gene silencing thereby preventing the attachment and entry of this infective agent into the human/host cells. This study will have a significant contribution and acts as a stepping stone in developing potential antiviral therapies against SARS COV-2.

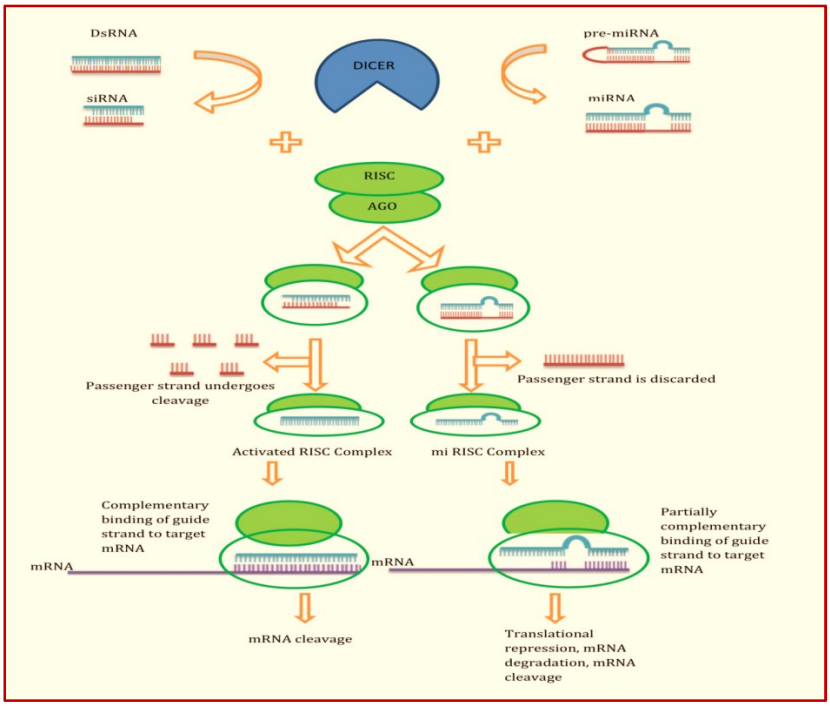

Figure 1: Schematic representation of RNAi Mechanism by siRNA and miRNA

METHODOLOGY

A flowchart of the methods followed for efficient RNAi designing is shown in **Figure 2**.

1. Retrieval of gene sequence

From NCBI Genbank database genes that encode for surface glycoprotein (Spike protein) from 10 different strains SARS CoV2 virus. Their accession numbers are NC_045512.2, MT192773.1, MT192759.1, MT188340.1, MT123293.2, MT184913.1, LC529905.1, MT066156.1, MT126808.1 and LC528233.1

2. ORF screening

From NCBI ORF Finder each of the gene sequences were screened for its open reading frames. A total 18 ORFs were found out of which ORF1 spans the entire gene sequence consisting of 3822 nucleotides and 1273 amino acids. ORF1 sequence was used for designing for RNAi molecules. **Figure 3** indicates the results obtained in the screening of gene sequences in Open Reading Frame Viewer.

3. Multiple sequence alignment and evolution analysis

Multiple sequence alignment (MSA) was carried out for the coding sequence of the 10 viral strains in CLUSTAL W tool in MEGA software (v6.06) where the evolutionary divergence of the strains was analysed by constructing a phylogenetic tree based on maximum likelihood algorithm where the value of bootstrapping was set to 500 **[15]**.

4. Design of RNAi molecule

To design target specific siRNA using siDirect 2.0 based on rules Ui-Tei Amarzguioui and Reynolds where the default melting temperature is below

21.5˚C for the siRNA duplex to eliminate off-target similarity **[16]**. The rules for designing effective siRNA are listed in **Table 1 [17-20]**. IDT miRNA webserver tool was used to design potential miRNA.

5. Search for off- target similarity

NCBI's BLAST standalone package was used to identify off-target binding with non-targeted organism's genome by setting parameters to BLOSUM 62 and expected thresholds value to 10 **[21]**.

6. Calculation of GC Content and prediction of secondary structures

The GC content for the predicted RNAi molecules was computed with DNA/RNA GC content calculator (http://www.endmemo.com/bio/gc.php).

RNA structure web server and mfold server were used for the prediction of secondary structures for the predicted RNAi molecules and calculation of the ΔG of folding at 37˚C **[22, 23]**.

7. Calculation of RNA–RNA interactions based on its thermodynamics

Using RNAcofold program thermodynamic interactions between the target and guide strand of siRNA were studied to compute hybridisation energy and base pairing based on McCaskill's partition function algorithm **[24]**. In a similar fashion RNA hybrid program was used for studying the thermodynamic interactions of predicted miRNAs **[25]**.

8. Heat capacity and concentration plot calculation

Heat capacity and concentration plotsfor the predicted RNAi molecules were computed using DINAMelt tool in UNAfold web server studies the melting profiles as a function of melting temperature (Tm) for a hybridized nucleic acid couple at equilibrium. The heat capacity plot reveals in detail the contributions of each entity to its ensemble heat capacity, on the other hand the concentration plot of Tm (Conc) which indicates that temperature of double-stranded molecules at which it achieves half of its maximum value **[26]**.

9. Prediction of secondary structures

Secondary structures formed between predicted RNAi guide strand and target were computed using RNA structure webserver **[22]**.

10. Validation of predicted RNAi

The validation of predicted RNAi was performed using DSIR tool where efficacy prediction was done based on the intrinsic features of RNAi **[27]**.

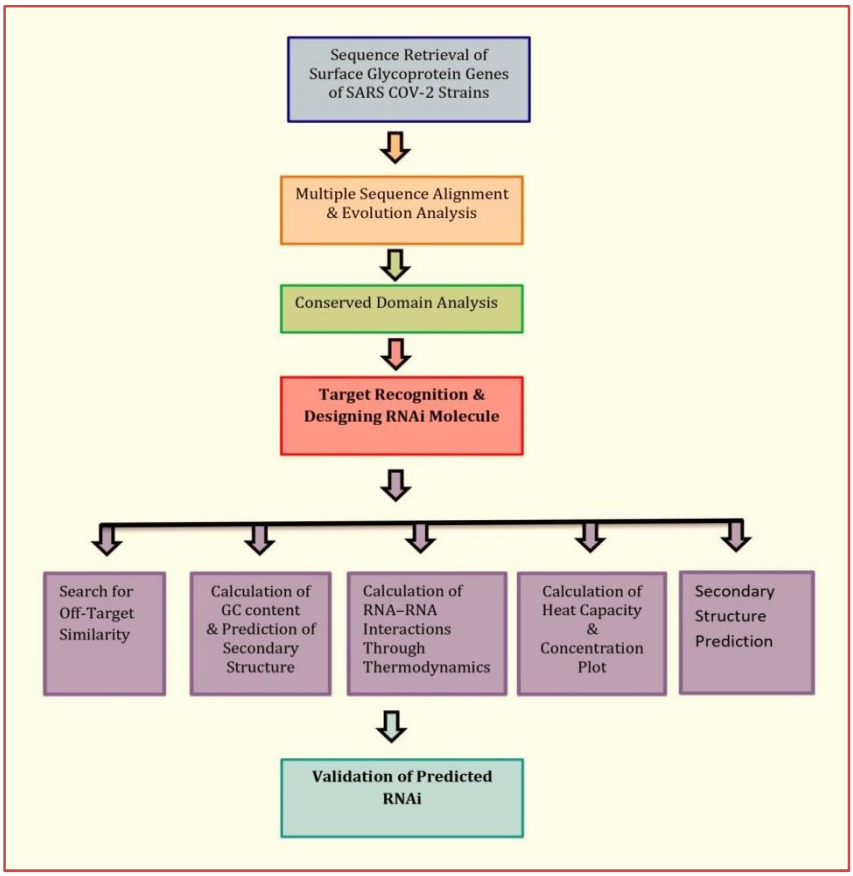

Figure 2: Methods followed for efficient RNAi designing

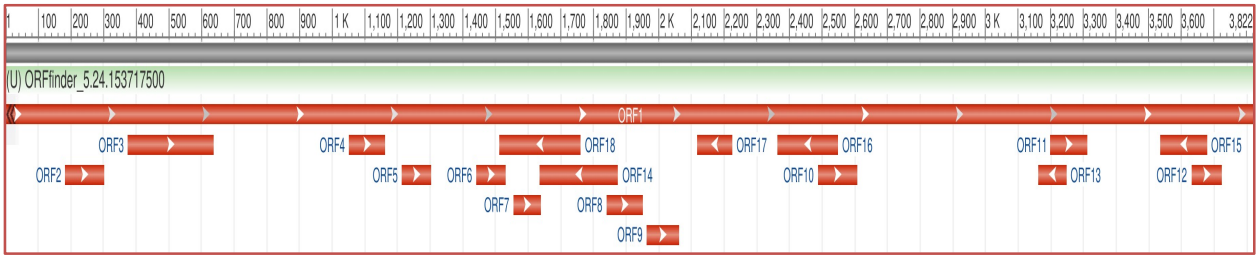

Figure 3: S gene in Open Reading Frame Viewer

Table 1: Rules for effective siRNA designing

Ui–Tei rules	Amarzguioui rules	Reynolds rules
1. A/U at the 5_ terminus of the sense strand 2. G/C at the 5_ terminus of the antisense strand 3. At least 4 A/U residues in the 5_ terminal 7 bp of sense strand 4. No GC stretch longer than 9nt	1. Duplex End A/U differential >0 2. Strong binding of 5_ sense strand 3. No U at position 1 4. Presence of A at position 6 5. Weak binding of 3_ sense strand 6. No G at position 19	1. Threshold for efficient siRNAs score = 6 2. Moderate to low (30%-52%) GC Content 3. At least 3 A/Us at positions 15-19 in sense strand 4. Lack of internal repeats(Tm−20◦C) 5. Presence of U at position ten of the sense strand 6. Absence of G at position 13 of the sense strand 7. Presence of A at position three of the sense strand

RESULTS & DISCUSSION

The S gene code for surface glycoproteins in coronaviruses therefore silencing of this gene results in termination of its essential functions thereby preventing it's entry into the host cells. In the present study gene sequences of 10 viral strains of SARS CoV2 were retrieved from NCBI and further posed to NCBI's ORF Finder tool so as to identify the coding sequences of S gene. The screening made it evident that amongst the 18 ORFs which are present in the coding sequence of S gene, the ORF1 spans the entire length of S gene. Subsequently, MSA was performed using CLUSTAL W (MEGA6.0) where all the ORF1 Sequences were aligned with each other, revealing 100% sequence similarity amongst the 10 sequences of ORF1. Evolutionary divergence of the ORF1 sequence was studied by generating a phylogenetic tree based on maximum likelihood approach that provides the probability of the sequences in an evolutionary model where the probability is measured as log function of likelihood where larger the number greater is the probability **[28]**. The evolutionary tree seen in **Figure 4** indicates that the viral sequences are highly conserved and therefore suitable for RNAi construction for wide spectrum of SARS CoV2 strains.

According to the UAR rules mentioned in **Table 1** the siDirect 2.0 tool predicted 42 potential siRNA duplexes where the GC content was maintained in the range of 30-60%. Similarly IDT tool yielded 58 miRNA duplexes. To reinsure the elimination of off-target binding in othernon-targeted organism, the RNAi sequences were run on BLAST tool against whole Genebankdatabase revealing no possible chances of off-target binding. The GC content calculations for selected RNAi molecules range from 30.95 - 40.47 **(Table 2)** and 28.846 - 34.615 **(Table 3)** for siRNA and miRNA respectively supporting the feasibility of the predicted RNAi molecules. Studies suggest lower GC content approximately in the range 31.6-57.9% result in higher RNAi efficacy **[29, 30]**. Prediction of secondary structures has shown an 80% elimination of non-functional siRNA sites **[31]**. Predicted MFE structures have a high positive predictive value for highly probable base pairing for RNA secondary structures based partition function **[32]**. Keeping these factor in mind the secondary structure their MFE and folding energies were computed using RNA cofold program for predicted siRNAs and miRNAs. Free energy of minimisation (MFE) refers to the equilibrium state where the molecule undergoes folding in its lowermost energy state **[33]**. The minimum free energy of selected RNAi molecules ranges from -23.20 to -26.10kcal/mol **(Table 2)** and -3.80 to-11.80kcal/mol

(Table 3) for siRNAs and miRNAs respectively.

The folding energy of guide strand of RNAi were in the range 0.40-2 **(Table 2)** and 1.6-2.6 **(Table 3)** for siRNAs and miRNAs respectively along with their secondary structures depicted in **Figure 5 and 6**.

After cleavage by RISC complex the guide strand of siRNA undergoes binding to target messenger RNA completely complimentary fashion. The thermo-dynamics of their RNA–RNA interactions is assumed as the total energy required for opening the binding site and the hybridisation energy of the heterodimer **[34]**. So, Gibbs free energy of binding for interactions between target messenger RNA and its predicted siRNA molecule is **[35]**:

$$\Delta G_{binding} = \Delta G_{AB} - \Delta G_{A} - \Delta G_{B}$$

Where ΔG_{AB} is the Gibbs free energy of heterodimeric structure formed by two sequences A and B. ΔG_{A} and ΔG_{B} represent free energy of the individual sequences. The free energy of binding of predicted siRNAs range from -29.5 to -33.8kcal/mol listed in the **Table 2**. In miRNA complementary binding with target mRNA takes place partially there binding energies are listed in **Table 3**.

The values for Tm(Cp) of predicted siRNA and miRNA range from 71.4-80.6˚C and 73.7-80.9˚C respectively which are listed in **Table 2 and Table 3**. Also Tm(Conc) values of predicted siRNA and miRNA range from 72.7 to 80.6 ˚C and 74.3 to 80.8 ˚C respectively. All the selected RNAi have high values of Tm listed in **Table 2 and Table 3**. The most stable secondary structures formed between the target strand and guide strand of selected RNAi with minimum free energy of binding. for DSIR tool was used to determine the inhibition efficacy of the predicted RNAi molecules where the thresold score is 90. Later based on all the parameter and free energy and Tm value, 16 of them were chosen to be the best probable RNAi molecules against the surfaceglycoprotein gene of SARS CoV2 virus. **Figure 7 and 8** show the secondary structures of the validated RNAi candidates for predicted miRNA and siRNA respectively.

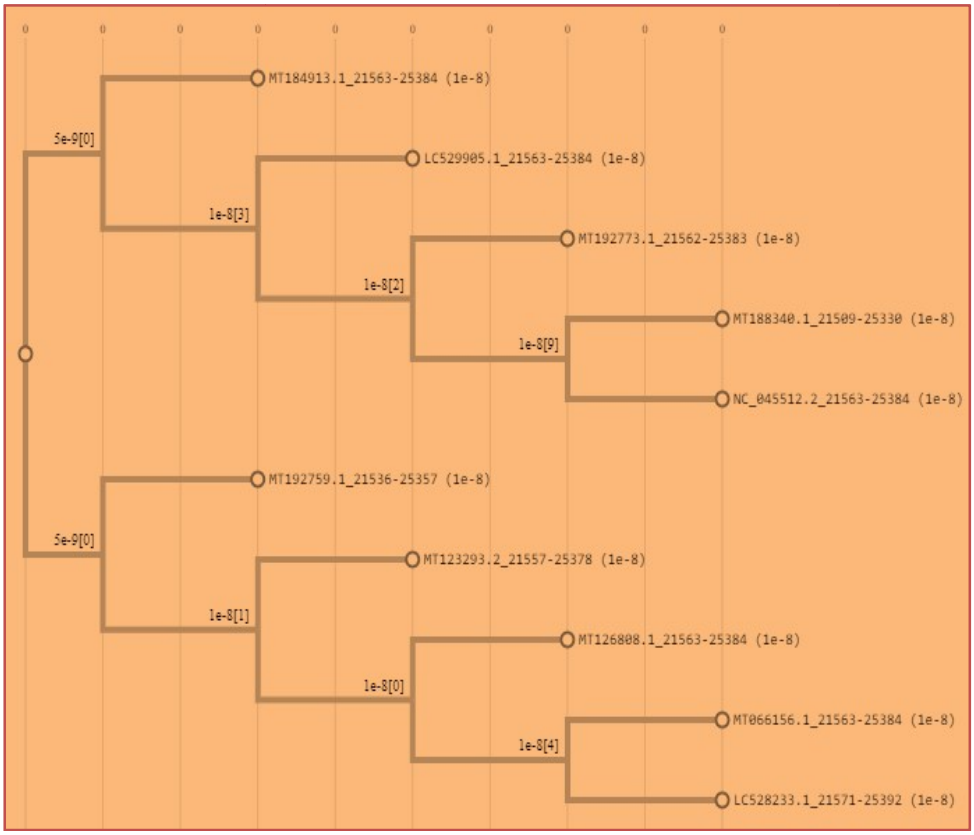

Figure 4: Phylogenetic tree of different strains of SARS CoV2 Virus

Table 2: Predicted siRNA and their properties

Predicted siRNA										
Position	Target	Guide (Antisense strand)	Passenger (Sense strand)	GC content (%)	MFE (kcal/mol)	ΔG binding (kcal/mol)	ΔG folding (kcal/mol)	Tm(Conc) °C	Tm(Cp) °C	DSIR Score
222-244	TGGTACTAAGAGGTTT GATAACC	UUAUCAAACCUCUU AGUACCA	GUACUAAGAGGUUUGAU AACC	35.71	-24.00	-32.6	0.50	76.5	77.9	90.7
567-589	TAGGGAATTTGTGTTTA AGAATA	UUCUUAAACACAAA UUCCCUA	GGGAAUUUGUGUUUAA GAAUA	28.57	-23.90	-29.7	2.10	74.2	75.4	99.8
890-912	CAGAAACAAAGTGTAC GTTGAAA	UCAACGUACACUUU GUUUCUG	GAAACAAAGUGUACGUU GAAA	35.71	-24.90	-32.8	0.50	76.7	77.8	97.1
1032-1054	CACCAGATTTGCATCTG TTTATG	UAAACAGAUGCAAA UCUGGUG	CCAGAUUUGCAUCUGUU UAUG	38.09	-26.10	-33.7	2	75.5	77.0	96.9
1244-1266	CTGGAAAGATTGCTGA TTATAAT	UAUAAUCAGCAAUC UUUCCAG	GGAAAGAUUGCUGAUUA UAAU	30.95	-24.20	-32.2	1.8	76.9	78.3	97.3
1295-1317	GCGTTATAGCTTGGAAT TCTAAC	UAGAAUUCCAAGCU AUAACGC	GUUAUAGCUUGGAAUUC UAAC	35.71	-24.40	-33.8	1.8	80.6	82.2	91
1611-1633	ATGTGTCAATTTCAACT TCAATG	UUGAAGUUGAAAUU GACACAU	GUGUCAAUUUCAACUUC AAUG	30.95	-23.20	-29.5	1.8	76.3	77.7	101.1
3438-3460	CTCATTCAAGGAGGAG TTAGATA	UCUAACUCCUCCUUG AAUGAG	CAUUCAAGGAGGAGUUA GAUA	40.476	-28.80	-36.6	0.40	73.9	75.0	91.8
3598-3620	CTCCAAGAACTTGGAAA GTATGA	AUACUUUCCAAGUU CUUGGAG	CCAAGAACUUGGAAAGU AUGA	38.095	-26.00	-33.8	1.9	75.2	71.4	92.7
3790-3812	GTGCTCAAAGGAGTCA AATTACA	UAAUUUGACUCCUU UGAGCAC	GCUCAAAGGAGUCAAAU UACA	38.095	-25.60	-33.7	1.9	72.7	73.6	92.1

Table 3: Predicted miRNA and their properties

Predicted miRNA										
Position	Target	Guide (Antisense strand)	Passenger (Sense strand)	GC content %	MFE (kcal/mol)	ΔG binding (kcal/mol)	ΔG folding (kcal/mol)	Tm(Conc) (°C)	Tm(Cp) (°C)	DSIR Score
1393-1418	AGAGAGATATTTC AACTGAAATCTA	AGAUUUCAGUUGAA AUAUCUCUCUCAA	GAGAGAGAUAUUU CAACUGAAAUCT	30.769	-11.00	-36.8	1.6	74.6	74.1	95.3
1394-1419	GAGAGATATTTCA ACTGAAATCTAT	UAGAUUUCAGUUGA AAUAUCUCUCUCA	AGAGAGAUAUUUC AACUGAAAUCTA	28.846	-11.00	-36.8	2.2	74.3	73.7	94.2
2432-2457	ACCAAGCAAGAG GTCATTTATTGAA	UCAAUAAAUGACCUC UUGCUUGGUUUU	AACCAAGCAAGAG GUCAUUUAUUGA	34.615	-3.80	-40.1	2.6	80.8	80.9	92.8
2433-2458	CCAAGCAAGAGG TCATTTATTGAAG	UUCAAUAAAUGACC UCUUGCUUGGUUU	ACCAAGCAAGAGG UCAUUUAUUGAA	34.615	-3.80	-39.8	2.6	79.4	79.2	91.6
2436-2461	AGCAAGAGGTCA TTTATTGAAGATC	AUCUUCAAUAAAUG ACCUCUUGCUUGG	AAGCAAGAGGUCA UUUAUUGAAGAT	34.615	-6.90	-37.4	2.2	77.3	77.4	92
2443-2468	GGTCATTTATTGA AGATCTACTTTT	AAAGUAGAUCUUCA AUAAAUGACCUCU	AGGUCAUUUAUUG AAGAUCUACUTT	28.846	-11.80	-35.8	1.9	74.7	74.0	93.7

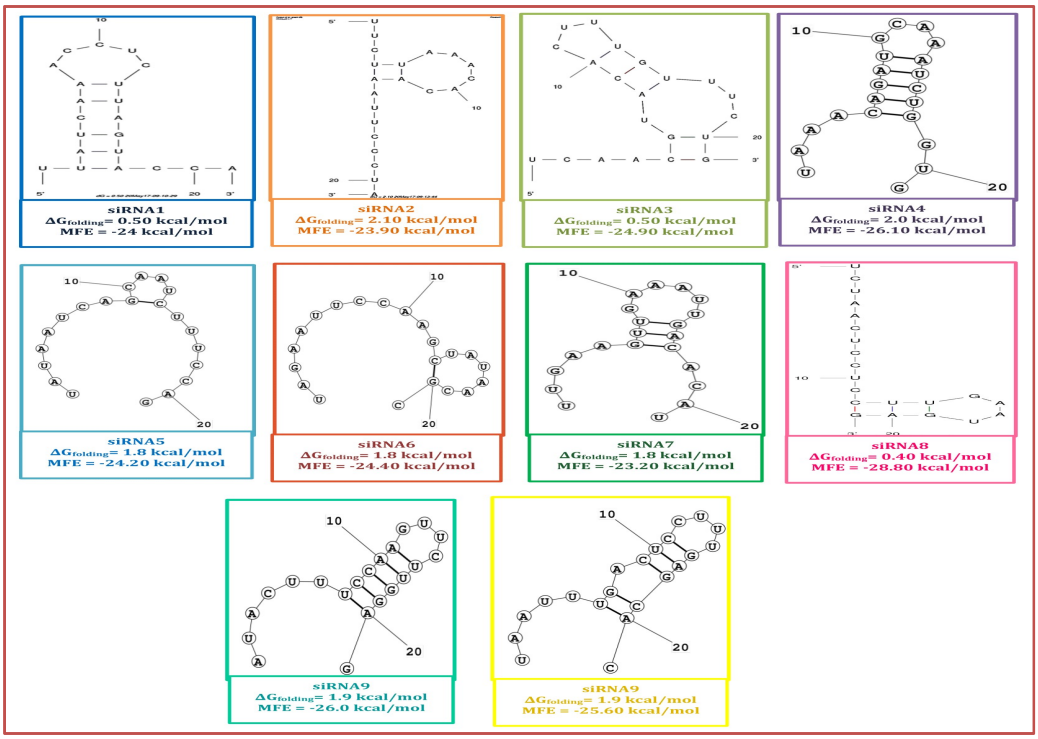

Figure 5: Secondary Structure of predicted siRNA along with their free energy of folding and MFE

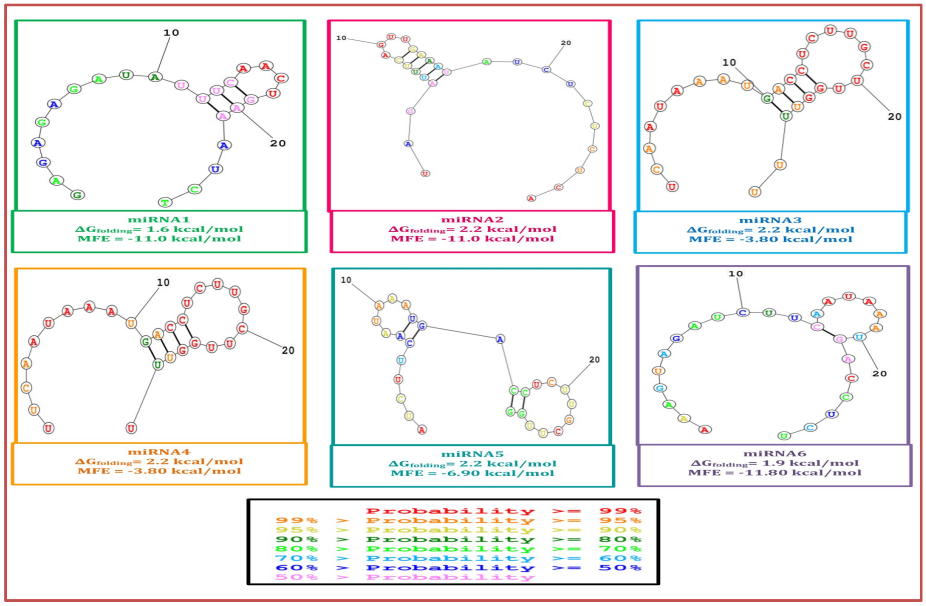

Figure 6: Secondary Structure of predicted miRNA along with their free energy of folding and MFE

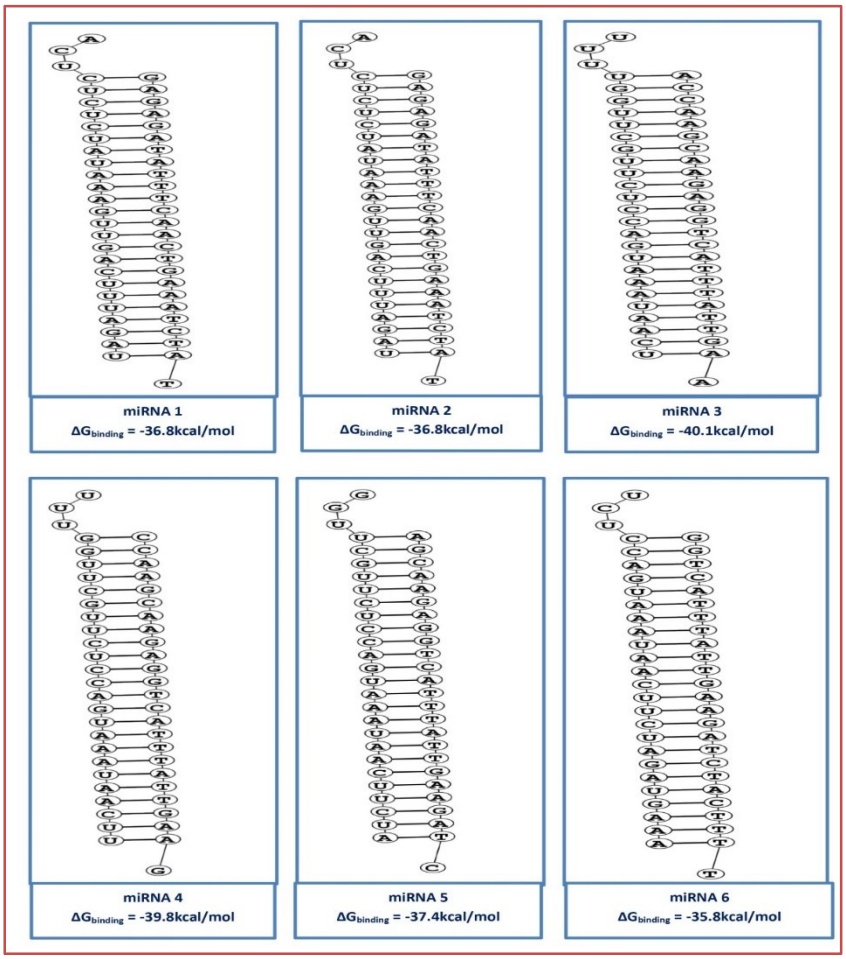

Figure 7: Secondary structures of predicted miRNA with target

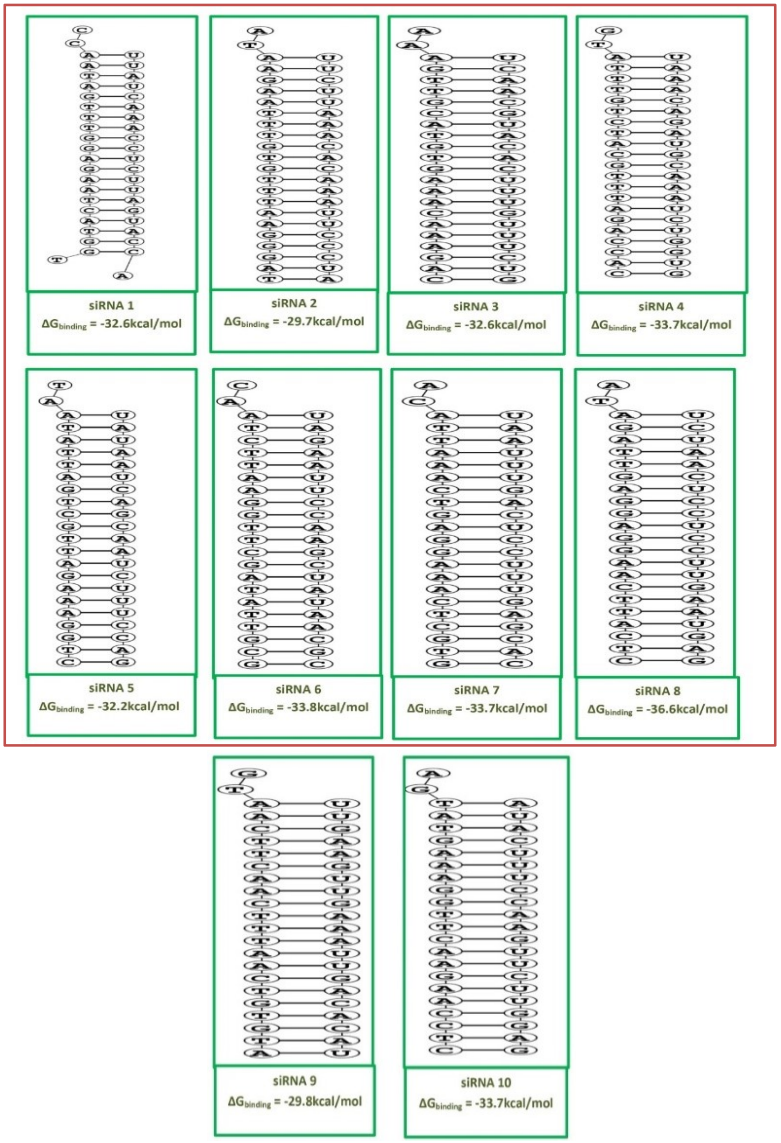

Figure 8: Secondary structures of predicted siRNA with target

CONCLUSIONS

In this study 10 SARS CoV2 strains each isolated from a different country are used to design 16 potential RNAi molecules targeting the Spike protein of SARS CoV2 which is aimed to render the virus incapable of attachment to host cells. These RNAi molecules have been screened through rigorous computational approaches to validate their gene silencing effect. Hence, it may facilitates vaccine development by utilizing RNAi as medium to block the access of the virus into the human host and may help the readers to effectively use the information for their research endeavours.

REFERENCES

[1] Guan WJ, Ni ZY, Hu Y, Liang WH, Ou CQ, He JX, Liu L, Shan H, Lei CL, Hui DS, Du B. Clinical characteristics of coronavirus disease 2019 in China. New

England journal of medicine. 2020 Apr 30; 382(18): 1708-20.

[2] Yang Y, Lu Q, Liu M, Wang Y, Zhang A, Jalali N, Dean N, Longini I, Halloran ME, Xu B, Zhang X. Epidemiological and clinical features of the 2019 novel coronavirus outbreak in China. MedRxiv. 2020 Jan 1.

[3] Song W, Gui M, Wang X, Xiang Y. Cryo-EM structure of the SARS coronavirus spike glycoprotein in complex with its host cell receptor ACE2. PLoS pathogens. 2018 Aug 13; 14(8): e1007236.

[4] Kogan A, Segel MJ, Ram E, Raanani E, Peled-Potashnik Y, Levin S, Sternik L. Acute Respiratory Distress Syndrome following Cardiac Surgery: Comparison of the American-European Consensus Conference Definition versus the Berlin Definition. Respiration. 2019; 97(6): 518-24.

[5] Agarwal A, Chen A, Ravindran N, To C, Thuluvath PJ. Gastro-intestinal and liver manifestations of COVID-19. Journal of Clinical and Experime-ntal Hepatology. 2020 Apr 1.

[6] Abbasi-Oshaghi E, Mirzaei F, Farahani F, Khodadadi I, Tayebinia H. Diagnosis and treatment of coronavirus disease 2019 (COVID-19): Laboratory, PCR, and chest CT imaging findings. International Journal of Surgery. 2020 May 15.

[7] D'Arienzo M, Coniglio A. Assessment of the SARS-CoV-2 basic reproduction number, R0, based on the early phase of COVID-19 outbreak in Italy. Biosafety and Health. 2020 Apr 2.

[8] Wu R, Wang L, Kuo HC, Shannar A, Peter R, Chou PJ, Li S, Hudlikar R, Liu X, Liu Z, Poiani GJ. An Update on Current Therapeutic Drugs Treating COVID-19. Current Pharmacology Reports. 2020 May 11:1.

[9] Kung HF, He ML, Zheng BJ, Guan Y, Lin MC, Peng Y, inventors; University of Hong Kong (HKU), assignee. Inhibition of SARS-associated coronavirus (SCoV) infection and replication by RNA interference. United States patent US 7, 129, 223. 2006 Oct 31.

[10] Hasan MM, Akter R, Ullah M, Abedin M, Ullah GM, Hossain M. A computational approach for predicting role of human micro-RNAs in MERS-CoV genome. Advances in bioinformatics. 2014; 2014.

[11] Lam JK, Chow MY, Zhang Y, Leung SW. siRNA versus miRNA

as therapeutics for gene silencing. Molecular Therapy-Nucleic Acids. 2015 Jan 1; 4: e252.

[12] Kim DH, Rossi JJ. Strategies for silencing human disease using RNA interference. Nature Reviews Genetics. 2007 Mar; 8(3): 173-84.

[13] Ha M, Kim VN. Regulation of microRNA biogenesis. Nature reviews Molecular cell biology. 2014 Aug; 15(8): 509-24.

[14] Valencia-Sanchez MA, Liu J, Hannon GJ, Parker R. Control of translation and mRNA degradation by miRNAs and siRNAs. Genes & development. 2006 Mar 1; 20(5): 515-24.

[15] Tamura K, Stecher G, Peterson D, Filipski A, Kumar S. MEGA6: molecular evolutionary genetics analysis version 6.0. Molecular biology and evolution. 2013 Dec 1; 30(12): 2725-9.

[16] Naito Y, Yoshimura J, Morishita S, Ui-Tei K. siDirect 2.0: updated software for designing functional siRNA with reduced seed-dependent off-target effect. BMC bioinformatics. 2009 Dec; 10(1): 392.

[17] Ui-Tei K, Naito Y, Takahashi F *et al.* Guidelines for the selection of highly effective siRNA sequences for mammalian and chick RNA interference. *Nucleic Acids Res.* 32(3), 936–948 (2004).

[18] Reynolds A, Leake D, Boese Q, Scaringe S, Marshall WS, Khvorova A. Rational siRNA design for RNA interference. *Nat. Biotechnol.* 22(3), 326 (2004).

[19] Amarzguioui M, Prydz H. An algorithm for selection of functional siRNA sequences. *Biochem. Biophys. Res. Comm.* 316(4), 1050–1058(2004).

[20] Ui-Tei K, Naito Y, Nishi K, Juni A, Saigo K. Thermodynamic stability and Watson–Crick base pairing in the seed duplex are major determinants of the efficiency of the siRNA-based off-target effect. *Nucleic Acids Res.* 36(22), 7100–7109 (2008).

[21] Johnson M, Zaretskaya I, Raytselis Y, Merezhuk Y, McGinnis S, Madden TL. NCBI BLAST: a better web interface. Nucleic AcidsRes. 36(Suppl. 2), W5–W9 (2008). (http://www.ncbi.nlm.nih.gov/blast)

[22] Bellaousov S, Reuter JS, Seetin MG, Mathews DH. RNAstructure: web servers for RNA secondary structure prediction and analysis. Nucleic acids research. 2013 Jul 1; 41(W1): W471-4.

[23] Zuker M. Mfold web server for nucleic acid folding and hybridization prediction. Nucleic acids research. 2003 Jul 1; 31(13): 3406-15.

[24] Bernhart SH, Tafer H, Mu¨ckstein U, Flamm C, Stadler PF,Hofacker IL (2006) Partition function and base pairing probabilities of RNA heterodimers. Algorithms Mol Biol 16: 1–3

[25] Rehmsmeier M, Steffen P, Ho¨chsmann M, Giegerich R (2006) Fast and effective prediction of microRNA/target duplexes. RNA10: 1507–1517

[26] Markham NR, Zuker M (2005) DINAMelt web server for nucleic acid melting prediction. Nucleic Acids Res 33: 577–581

[27] Filhol O, Ciais D, Lajaunie C, Charbonnier P, Foveau N, Vert JP, Vandenbrouck Y. DSIR: assessing the design of highly potent siRNA by testing a set of cancer-relevant target genes. PloS one. 2012; 7(10).

[28] Yang Z. Phylogenetic analysis by maximum likelihood (PAML).

[29] Liu Y, Chang Y, Zhang C, Wei Q, Chen J, Chen H, Xu D. Influence of mRNA features on siRNA interference efficacy. Journal of bioinformatics and computational biology. 2013 Jun 8; 11(03): 1341004.

[30] Chan CY, Carmack CS, Long DD, Maliyekkel A, Shao Y, Roninson IB, Ding Y. A structural interpretation of the effect of GC-content on efficiency of RNA interference. BMC bioinformatics. 2009 Jan 1; 10(S1): S33.

[31] Heale BS, Soifer HS, Bowers C, Rossi JJ. siRNA target site secondary structure predictions using local stable substructures. Nucleic acids research. 2005 Jan 1; 33(3): e30-.

[32] Mathews DH. Using an RNA secondary structure partition function to determine confidence in base pairs predicted by free energy minimization. Rna. 2004 Aug 1; 10(8): 1178-90.

[33] Ding Y, han CY, Lawrence CE (2005) RNA secondary structure prediction by centroids in a Boltzmann weighted ensemble. RNA 11: 1157–1166

[34] Muckstein U, Tafer H, Hackermuller J, Bernhart SB, Stadler F, Hofacker IL (2006) Thermodynamics of RNA–RNA binding. Bioinformatics 22: 1177–1182

[35] Bernhart SH, Tafer H, Mu¨ckstein U, Flamm C, Stadler PF, Hofacker IL (2006) Partition function and base pairing probabilities of RNA heterodimers. Algorithms Mol Biol 16: 1–3.